The Journal of Pathology: Clinical Research
J Path: Clin Res January 2018; **4:** 19–25
Published online 5 October 2017 in Wiley Online Library (wileyonlinelibrary.com). DOI: 10.1002/cjp2.84

BRIEF DEFINITIVE REPORT

Optimization of commercially available Zika virus antibodies for use in a laboratory-developed immunohistochemical assay

Brigid C Bollweg, Luciana Silva-Flannery, Pamela Spivey and Gillian L Hale*

Infectious Diseases Pathology Branch, Centers for Disease Control and Prevention, Atlanta, GA, USA

**Correspondence to: Gillian L Hale, Infectious Diseases Pathology Branch, Centers for Disease Control and Prevention, 1600 Clifton Rd NE, MS: G32, Atlanta, GA 30329-4027, USA. E-mail: cwx4@cdc.gov*

Abstract

Zika virus (ZIKV) infection during pregnancy can cause adverse fetal outcomes and severe irreversible congenital birth defects including microcephaly. Immunohistochemistry (IHC) is a valuable diagnostic tool for detecting ZIKV antigens in tissues from cases of fetal loss in women infected with ZIKV, and for providing insights into disease pathogenesis. As a result, there is increasing demand for commercially available ZIKV antibodies for use in IHC assays. ZIKV antibodies were selected and obtained from commercial sources to include both mouse and rabbit hosts, and a variety of antigenic targets. Pretreatment conditions and antibody concentrations resulting in optimal immunohistochemical staining were determined using ZIKV cell control and polymerase chain reaction (PCR)-confirmed ZIKV case control material (fetal brain tissue). Cross-reactivity of the antibodies against other flaviviruses (dengue virus serogroups 1–4, yellow fever virus, Japanese encephalitis virus, West Nile virus) and chikungunya virus was also evaluated. Immunostaining using the commercially available antibodies was compared to a previously validated ZIKV IHC assay used for primary diagnosis. Four antibodies demonstrated optimal staining similar to the previously validated ZIKV IHC assay. Two of the four antibodies cross-reacted with dengue virus, while the other two antibodies showed no cross-reactivity with dengue, other flaviviruses, or chikungunya virus. Differences in the cross-reactivity profiles could not be entirely explained by the antigenic target. Commercially available ZIKV antibodies can be optimized for use in IHC testing to aid in ZIKV diagnostic testing and an evaluation of tissue tropism.

Keywords: Zika virus; immunohistochemistry; antibody; pathology; placenta; fetal demise; microcephaly

Received 5 June 2017; Revised 26 September 2017; Accepted 2 October 2017

No conflicts of interest were declared.

Introduction

Zika virus (ZIKV) belongs to the *Flaviviridae* family of RNA viruses and is borne by mosquitoes like the related dengue, yellow fever, West Nile, and Japanese encephalitis viruses [1]. The majority of infections may go unnoticed, while a smaller proportion of otherwise healthy non-pregnant adults may experience a self-limited dengue-like illness characterized by fever, rash, and arthralgia [2]. However, unlike other flaviviruses, it is the well-recognized potential of ZIKV to cause severe congenital birth defects including microcephaly that has brought this virus to the forefront of a public health emergency [3,4]. The association between microcephaly and autochthonous ZIKV infection became manifest in Brazil in 2015 with the significant concomitant increase in both [3]. Yet, perhaps one of the most significant contributions to our understanding of ZIKV as the causative agent of congenital birth defects was the microscopic visualization and localization of viral antigens and RNA in affected fetal brain tissues by immunohistochemistry (IHC) and *in situ* hybridization, respectively [10–12].

In the initial stages of the disease outbreak, public health laboratories primarily performed diagnostic testing, but as the disease epidemic has grown, there has been an exponential rise in studies seeking to elucidate the mechanism of congenital ZIKV syndrome [5,6]. However, the diagnosis of ZIKV by serologic testing is challenging, particularly in areas where related viruses, such as dengue and yellow fever, co-circulate [6]. Tissue-based diagnostic modalities have the advantage of prolonged opportunities for detection, whereas transient viremia challenges efforts at nucleic acid testing in serologic specimens [6]. IHC is a particularly valuable tool for investigating tissue tropisms and the

Table 1. Commercially available antibodies optimized for IHC: antibody source, characteristics, and pretreatment conditions

Antibody	Antibody name (target antigen)	Source	Catalog #	Host, type	Conditions tested*			Optimal conditions
ARI-A	Zika virus NS1 SQab1609	Arigobio	ARG65781	Mouse, monoclonal	1:250 PK 1:250 AR	1:500 PK 1:500 AR 1:500 ARE	1:1000 PK 1:1000 AR	1:500 AR
BIO-B	Zika envelope protein 0302156	BioFront	BF-1176-56	Mouse, monoclonal	1:100 PK 1:100 ARE	1:500 PK 1:500 ARE	1:1000 PK 1:1000 ARE	1:100 ARE
GTX-C	Zika virus NS1 protein	GeneTex	GTX13307	Rabbit, polyclonal	1:100 PK 1:100 ARE	1:500 PK 1:500 ARE	1:1000 PK 1:1000 ARE	1:500 ARE
GTX-D	Zika virus NS2B protein	GeneTex	GTX13308	Rabbit, polyclonal	1:100 PK 1:100 ARE	1:500 PK 1:500 ARE	1:1000 PK 1:1000 ARE	1:500 ARE

*Primary antibody concentration is indicated first, followed by pretreatment: PK (proteinase K), AR (antigen retrieval, citrate buffer), ARE (antigen retrieval, EDTA buffer).

pathogenesis of ZIKV in patients and in animal models of infection. In fetal tissues, ZIKV antigens have been detected by IHC in the brain in areas of microcalcification and gliosis, in the retina, and in placental tissues (Hofbauer cells) [5,7]. Yet, there are overall only few reports of utilizing ZIKV IHC in diagnosis, and the primary antibodies used in most of the published studies are broadly non-specific, anti-flavivirus antibodies, or are not commercially available [7–9].

Thus, there is a growing demand for commercially available ZIKV antibodies for use in IHC assays [6]. A variety of ZIKV antibodies targeting non-structural and structural ZIKV epitopes can now be obtained commercially and adapted for use in laboratory-developed assays. CDC's Infectious Diseases Pathology Branch (IDPB) is uniquely positioned to evaluate ZIKV antibodies by IHC, given early involvement in the ZIKV outbreak [10,11] and ample availability of cell and PCR-confirmed case control material, as well as long-standing experience in using IHC in the diagnosis of emerging infections.

In this study, IDPB obtained commercially available ZIKV antibodies for optimization in an IHC assay with the goal of sharing data on optimal pretreatment conditions, antibody concentrations, and antibody cross-reactivity profiles. Formalin-fixed, paraffin-embedded cell control and PCR-confirmed congenital ZIKV case material was used in assay development. The staining characteristics of each antibody were compared to IDPB's previously validated primary diagnostic ZIKV IHC assay [10].

Materials and methods

Cell and case control material

The ZIKV-infected cell control used in assay development was derived from Vero E6 kidney cells inoculated with ZIKV, harvested, fixed in formalin, and embedded in paraffin wax. Brain tissue from a previously tested and confirmed congenital ZIKV case was used as a positive case control; established ZIKV IHC and PCR assays had been used to confirm the diagnosis [10,12]. The case control was a 2-month-old female born at 38-weeks' gestation with microcephaly and other malformations. Morphologic features were typical of congenital ZIKV syndrome [5] and included cortical thinning, gliosis, and microcalcifications.

Other cell controls used for cross-reactivity analysis included yellow fever virus, dengue virus (serogroups 1–4), West Nile virus, and chikungunya virus. A historic case control of Japanese encephalitis in an infected cynomolgus monkey was used for evaluating reactivity with this virus. We note that positive staining for Japanese encephalitis and evidence of cross-reactivity in tissue sections would need to demonstrate staining in neurons in necrotic foci of the spinal cord.

Uninfected Vero E6 cells were used as negative cell control material. Previously tested neonatal brain autopsy tissues negative for ZIKV by IHC and PCR testing were used as negative case control material.

The tissue samples were submitted to CDC for routine diagnostic testing during the ZIKV outbreak; the secondary use of these tissue samples was outside the scope of institutional review board (IRB) review requirements, as it did not involve human subjects. Specifically, the project was classified as research not involving human subjects per 45 CFR 46.102(f), and IRB review was not required.

Antibodies

ZIKV antibodies were selected from different companies to include a variety of target antigens [envelope, non-structural proteins (NS)], and different animal hosts (mouse, rabbit). The antibody sources, catalogue numbers, host, species, and target characteristics are listed in Table 1. The staining characteristics for each antibody were compared to IDPB's previously validated ZIKV IHC assay, which uses a mouse polyclonal antibody that was kindly provided by CDC's Division of

Table 2. Cross-reactivity profile of commercially available ZIKV antibodies tested by IHC against other flaviviruses and chikungunya virus (sg: serogroup; neg: negative; pos: positive)

Antibody	Yellow fever cells	WNV cells	Dengue (sg 1) cells	Dengue (sg 2) cells	Dengue (sg 3) cells	Dengue (sg 4) cells	Japanese encephalitis case	Chikungunya cells
ARI-A	Neg	Neg	Neg	Neg	Neg	Neg	Neg	Neg
BIO-B	Pos	Neg	Pos	Pos	Pos	Pos	Neg	Neg
GTX-C	Pos	Pos	Pos	Pos	Pos	Pos	Neg	Pos
GTX-D	Neg	Neg	Neg	Neg	Neg	Neg	Neg	Neg

Vector-Borne Diseases at Fort Collins and was derived from hyperimmune mouse ascitic fluid [10].

Immunohistochemistry

Immunohistochemical assays were performed using an indirect immuno-alkaline phosphatase detection methodology [12]. All steps of the staining procedure excluding heat-induced epitope retrieval (HIER) were performed at room temperature. In brief, 4 μm tissue sections of Zika-infected cell control or Zika-infected brain specimens were placed on slides. The sections were deparaffinized in three changes of xylene for 5, 3, and 1 min, respectively. Slides were rehydrated through graded alcohol solutions as follows: two changes of 100% ethanol for 2 and 1 min, respectively, followed by a 1 min incubation in 95% ethanol and subsequently 70% ethanol. Slides were rinsed with 1X Tris-buffered saline with Tween 20 (1X TBS-T) (Thermo Fisher Scientific, Waltham, MA, USA) before staining. Colorimetric detection of attached antibodies was performed using the Mach 4 AP Polymer kit (Biocare Medical, Concord, CA, USA). The optimal pretreatment conditions were evaluated using HIER with either citrate (Reveal, Biocare Medical) or EDTA-based buffers (Biocare Medical) on the Biocare NxGen decloaker (110 °C for 15 min), or tissue sections were digested with 0.1 mg/ml Proteinase K (Roche, Indianapolis, IN, USA) in 0.6M Tris/0.1% $CaCl_2$ for 15 min. Slides were rinsed in 1X TBS-T between each step of the staining procedure. All slides were then blocked in Background Punisher (Biocare Medical) for 10 min and incubated with a variety of anti-ZIKV-primary antibodies, for 30 min at various dilutions (Table 1). Antibodies were diluted in LabVision Ultra Clean Diluent (Thermo Fisher Scientific). Mach 4 Probe was applied for 10 min for mouse antibodies, followed by Mach 4 AP polymer for 15 min (Biocare Medical). For rabbit antibodies, the Mach 4 Probe was omitted and slides were incubated for 30 min with Mach 4 AP Polymer, according to manufacturer recommendations. The antibody/polymer conjugate was visualized by applying Fast Red Chromogen dissolved in Naphthol Phosphate (Thermo Fisher Scientific) substrate buffer to tissue sections for 20 min, after which they were rinsed in deionized water to quench chromogen precipitation. Appropriate negative control serum was run in parallel for each slide (normal rabbit serum, 1:1000, CDC laboratories; normal mouse serum, 1:1000, Jackson ImmunoResearch, West Grove, PA, USA, catalog #015-000-001). Slides were counterstained in Mayer's hematoxylin (Polyscientific, Bay Shore, NY, USA) and blued in lithium carbonate (Polysciences, Inc., Warrington, PA, USA). Slides were then coverslipped with aqueous mounting medium (Polysciences, Inc.).

Immunostaining was evaluated using a 5-point intensity scale (0–4). Optimal conditions were considered those that yielded a staining intensity of 4 in an appropriate distribution within infected cells or tissues, and with minimal background staining.

To determine the cross-reactivity profile of the antibodies, each commercially available ZIKV antibody was tested against dengue virus (serogroups 1–4), West Nile virus, Japanese encephalitis virus, yellow fever virus, and chikungunya virus using the established optimal conditions (Table 2). Chikungunya virus belongs to the family *Togaviridae* but shares a similar geographic distribution and clinical presentation to dengue and ZIKV [6,13,14], and therefore was included in the cross-reactivity analysis.

Results and discussion

Among the commercially available antibodies tested, pretreatment conditions resulting in optimal immunohistochemical staining of cell and case control material were determined for four antibodies (Table 1). The staining characteristics of each antibody are presented in Figures 1 and 2, using ZIKV-infected cell and case control material, respectively. High resolution version of these figures is provided as supplementary material, Figures S1 and S2, respectively. The staining quality was generally similar to a previously validated ZIKV IHC assay used in primary ZIKV diagnosis (Figures 1B–F and 2B–F) [10–12]. Each of the commercial antibodies showed intense, discrete red granular staining in a perinuclear distribution in neural cells, which was particularly

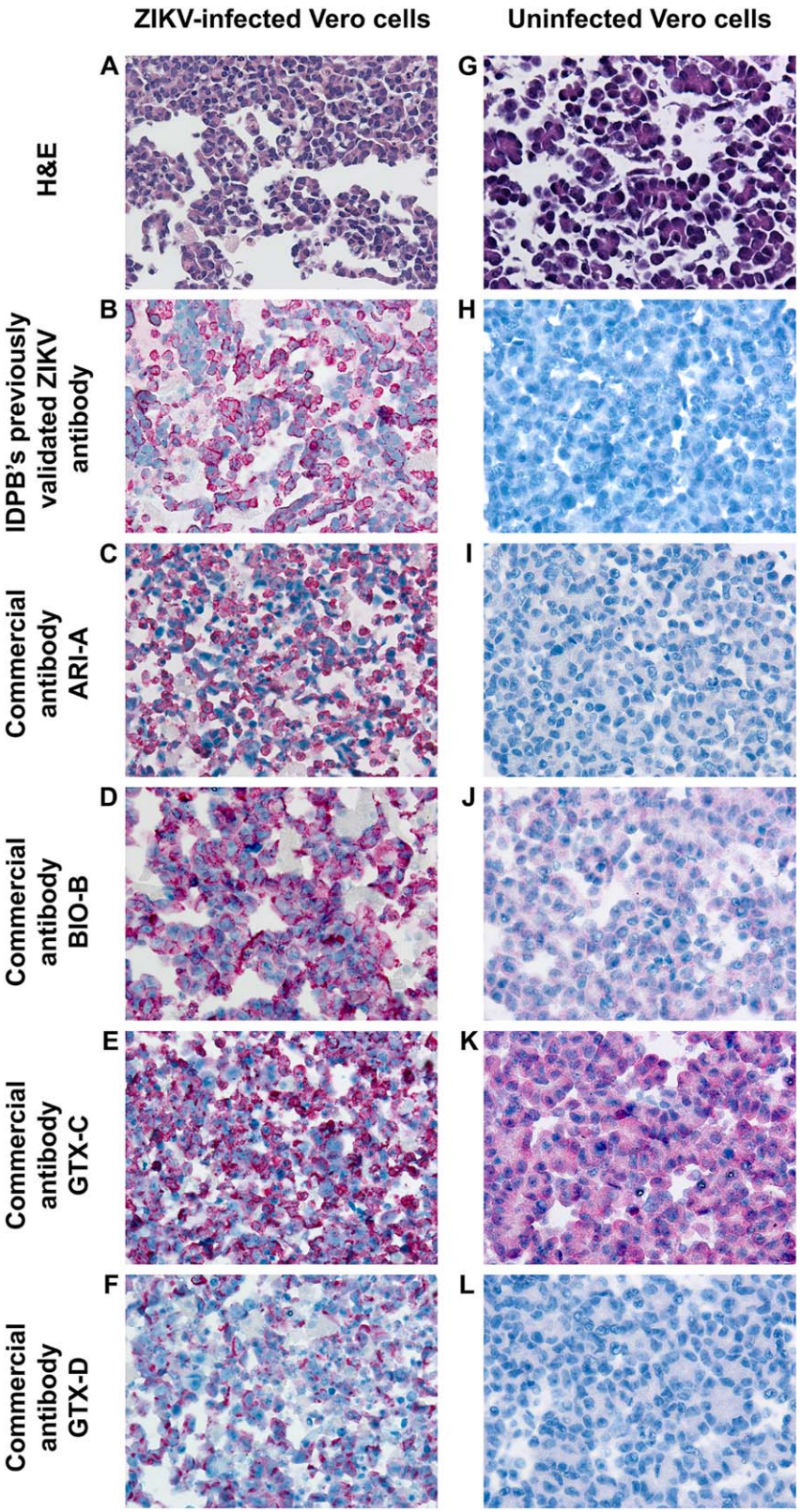

Figure 1. A comparison of immunostaining between commercially available ZIKV antibodies in ZIKV-infected Vero cells (A–F) and uninfected Vero cells (G–L). Objective magnification, 40X. A high resolution version of this figure is available in supplementary material, Figure S1.

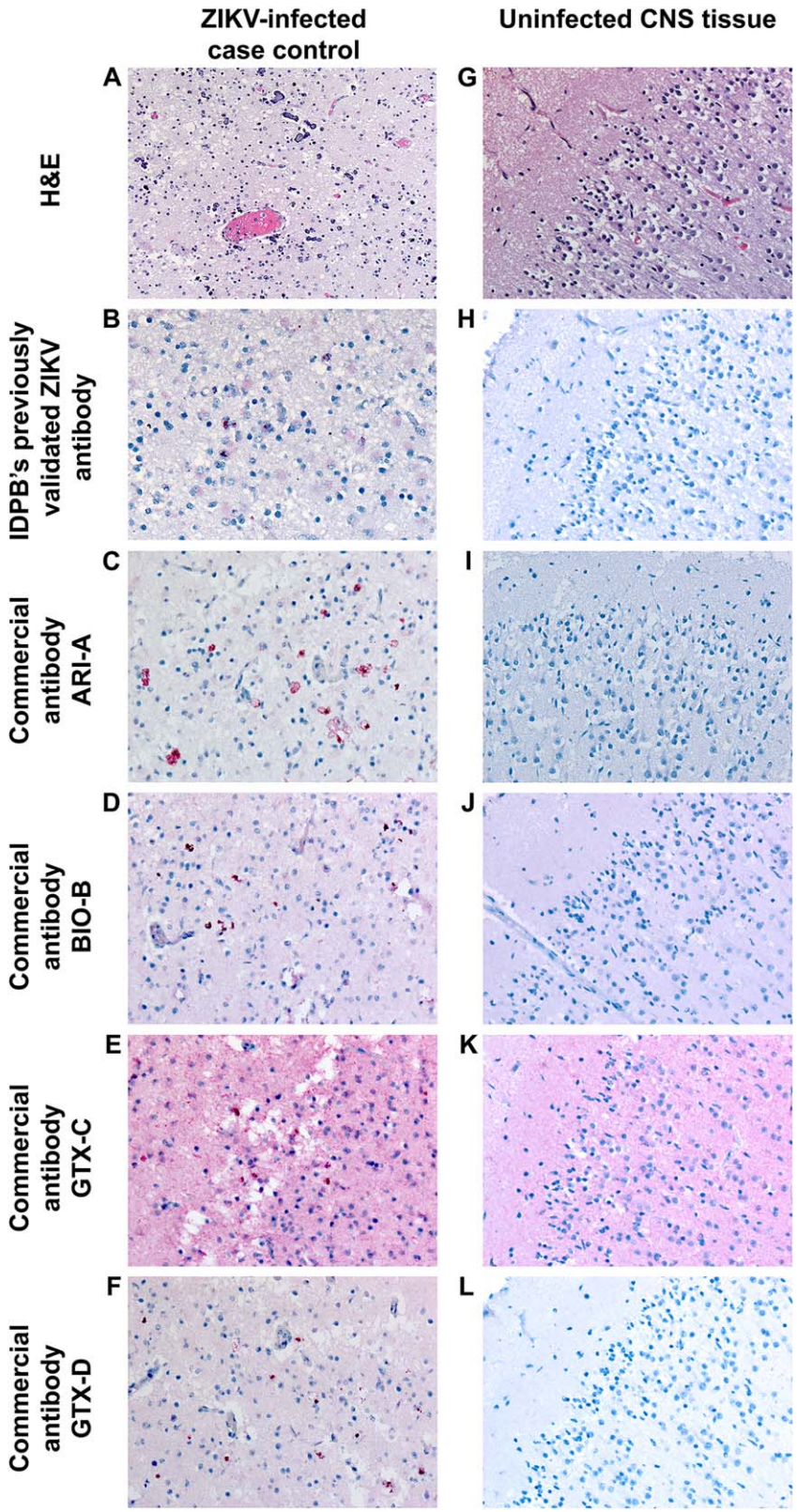

Figure 2. A comparison of immunostaining between the commercially available ZIKV antibodies using ZIKV-infected case control (A–F) and uninfected CNS tissue (G–L). Objective magnification, 20X. A high resolution version of this figure is available in supplementary material, Figure S2.

prominent in association with calcifications, as would be expected (Figure 2B–F) [10]. Images of antibody staining on uninfected Vero cells and ZIKV-uninfected brain tissue are also provided for evaluation of background staining (Figures 1H–L and 2H–L, respectively).

Non-specific staining, defined as a diffuse 'blush' in background tissues across different cell types was also observed to various degrees. Antibody BIO-B showed mild background staining in cells and tissues (Figures 1J and 2J), while prominent background staining was observed for antibody GTX-C (best appreciated in both uninfected Vero cells and uninfected CNS tissue, Figures 1K and 2K). Virtually, no background staining was seen with antibodies ARI-A (Figures 1I and 2I) and GTX-D (Figures 1L and 2L). We note that background staining may vary between laboratories depending upon duration of tissue fixation, pretreatment conditions, antibody host and dilution, blocking reagents, and colorimetric detection system; rabbit polyclonal antibodies such as GTX-C, for example, are known to be associated with higher background than mouse antibodies [15–18].

The results of cross-reactivity testing are displayed in Table 2 and supplementary material, Figures S3 and S4. Two of the four optimized antibodies (BIO-B and GTX-C) demonstrated cross-reactivity with all four dengue virus serotypes, while two of the antibodies (ARI-A and GTX-D) did not demonstrate cross-reactivity with dengue virus (serogroups 1–4), other flaviviruses (yellow fever, West Nile, Japanese encephalitis) or with chikungunya virus. Some nonspecific staining of few scattered cells (Supplementary figure 4M) and background uninfected tissue was identified in the yellow fever cell control with antibody GTX-D; however, the antibody was subsequently tested against yellow fever case control tissue and was unequivocally negative. Of note, the results of cross reactivity testing with ARI-A in tissue are supported by ancillary testing; according to the manufacturer of ARI-A (Arigobio product data sheet), no cross-reactivity was detected between this antibody and the NS1 proteins of dengue virus (serogroups 1–4) or chikungunya virus. Antibody BIO-B, a mouse monoclonal antibody that targets a recombinant Zika envelope protein [19], showed a mixed cross-reactivity profile, with staining in dengue virus and yellow fever virus cells, but without staining in West Nile, Japanese encephalitis, and chikungunya virus controls. In the Japanese encephalitis virus control tissue, non-specific staining was observed with antibodies BIO-B and GTX-C (supplementary material, Figures S4G,K, respectively); however, no immunostaining was seen in neurons in a distribution similar to the positive control with any of the antibodies. Antibody GTX-C cross-reacted with each of the flaviviruses (except Japanese encephalitis virus) as well as chikungunya virus and was therefore the most cross-reactive among the four commercially available antibodies tested.

The structural homology between the flaviviruses is a well-known challenge in the development of specific diagnostic modalities and can be considered in understanding the differences in cross-reactivity profiles. Like other flavivirus genomes, ZIKV encodes a single polyprotein that is processed in the cytoplasm of infected cells into three structural proteins (envelope, membrane precursor, capsid) and seven non-structural proteins (NS1, NS2a, NS2b, NS3, NS4a, NS4b, and NS5); and there is considerable overlap in the structural and non-structural proteins among flaviviruses [1,6,20]. The RNA genome of chikungunya virus similarly encodes four nonstructural and four structural proteins, and there are some similarities with ZIKV with respect to envelope protein folding [21].

However, differences in the cross-reactivity profiles of the antibodies cannot be entirely explained by the target antigen. For example, both ARI-A and GTX-C were raised against NS1, but showed different cross-reactivity profiles (Table 2). Rather, the differences may be explained by antibody host factors as antibody ARI-A is a mouse monoclonal antibody whereas GTX-C is a rabbit polyclonal antibody. Further evaluation of cross-reactivity among the viruses can be performed by individual laboratories.

In summary, herein we describe the optimization of IHC staining conditions, staining pattern, and cross-reactivity profiles for four commercially available ZIKV antibodies. Each of the antibodies displayed immunostaining similar to what was observed using IDPB's previously validated ZIKV IHC assay. Depending on the intended utility of antibodies used in IHC, the development of a specific ZIKV assay may be ideal for excluding other related flaviviruses.

We note that this study is not an exhaustive exploration of all currently available commercial antibodies, nor do the findings represent an endorsement for particular antibodies. Rather, these results may serve as a guide for laboratories seeking to develop their own ZIKV IHC testing protocol for the purposes of diagnostics and research activities. Depending on the specificity desired by the testing laboratory, each of these antibodies may have some utility.

Acknowledgements

The authors would like to acknowledge Dr. Sherif Zaki and IDPB staff pathologists for supporting this study, IDPB's histotechnologists for their contribution to block and slide preparation, Dr. Julu Bhatnagar and

IDPB's molecular team for PCR testing of case control material, and Dominique Rollin for her preparation of ZIKV-infected cell control material.

Author contributions statement

BB: performed immunohistochemical assay development for each of the commercially available antibodies, authored Materials and Methods and tables, and critically evaluated the manuscript; LF, PS: contributed to assay development and critical review of the manuscript; GH: selected ZIKV antibodies for acquisition and evaluation, selected ZIKV control material for testing, evaluated immunohistochemical staining characteristics of each antibody on prepared slides, and prepared introduction, results and discussion, and images for the manuscript.

The findings and conclusions in this report are those of the authors and do not necessarily represent the official position of the Centers for Disease Control and Prevention.

References

1. Gould EA, Solomon T. Pathogenic flaviviruses. *Lancet* 2008; **371:** 500–509.
2. Duffy MR, Chen TH, Hancock WT, *et al*. Zika virus outbreak on Yap Island, Federated States of Micronesia. *N Engl J Med* 2009; **360:** 2536–2543.
3. Rasmussen SA, Jamieson DJ, Honein MA, *et al*. Zika virus and birth defects–reviewing the evidence for causality. *N Engl J Med* 2016; **374:** 1981–1987.
4. Rubin EJ, Greene MF, Baden LR. Zika virus and microcephaly. *N Engl J Med* 2016; **374:** 984–985.
5. Ritter JM, Martines RB, Zaki SR. Zika virus: pathology from the pandemic. *Arch Pathol Lab Med* 2017; **141:** 49–59.
6. Landry ML, St George K. Laboratory diagnosis of Zika virus infection. *Arch Pathol Lab Med* 2017; **141:** 60–67.
7. Kawiecki AB, Mayton EH, Dutuze MF, *et al*. Tissue tropisms, infection kinetics, histologic lesions, and antibody response of the MR766 strain of Zika virus in a murine model. *Virol J* 2017; **14:** 82.
8. Noronha L, Zanluca C, Azevedo ML, *et al*. Zika virus damages the human placental barrier and presents marked fetal neurotropism. *Mem Inst Oswaldo Cruz* 2016; **111:** 287–293.
9. Azevedo RS, Araujo MT, Martins Filho AJ, *et al*. Zika virus epidemic in Brazil. I. Fatal disease in adults: clinical and laboratorial aspects. *J Clin Virol* 2016; **85:** 56–64.
10. Martines RB, Bhatnagar J, de Oliveira Ramos AM, *et al*. Pathology of congenital Zika syndrome in Brazil: a case series. *Lancet* 2016; **388:** 898–904.
11. Martines RB, Bhatnagar J, Keating MK, *et al*. Notes from the field: evidence of Zika virus infection in brain and placental tissues from two congenitally infected newborns and two fetal losses–Brazil, 2015. *MMWR Morb Mortal Wkly Rep* 2016; **65:** 159–160.
12. Bhatnagar J, Rabeneck DB, Martines RB, *et al*. Zika virus RNA replication and persistence in brain and placental tissue. *Emerg Infect Dis* 2017; **23:** 405–414.
13. Jain J, Mathur K, Shrinet J, *et al*. Analysis of coevolution in non-structural proteins of chikungunya virus. *Virol J* 2016; **13:** 86.
14. Furuya-Kanamori L, Liang S, Milinovich G, *et al*. Co-distribution and co-infection of chikungunya and dengue viruses. *BMC Infect Dis* 2016; **16:** 84.
15. Buchwalow I, Samoilova V, Boecker W, *et al*. Non-specific binding of antibodies in immunohistochemistry: fallacies and facts. *Sci Rep* 2011; **1:** 28.
16. Miller MA, Ramos-Vara JA, Kleiboeker SB, *et al*. Effects of delayed or prolonged fixation on immunohistochemical detection of bovine viral diarrhea virus type I in skin of two persistently infected calves. *J Vet Diagn Invest* 2005; **17:** 461–463.
17. Ramos-Vara JA. Technical aspects of immunohistochemistry. *Vet Pathol* 2005; **42:** 405–426.
18. Vilches-Moure JG, Ramos-Vara JA. Comparison of rabbit monoclonal and mouse monoclonal antibodies in immunohistochemistry in canine tissues. *J Vet Diagn Invest* 2005; **17:** 346–350.
19. Larocca RA, Abbink P, Peron JP, *et al*. Vaccine protection against Zika virus from Brazil. *Nature* 2016; **536:** 474–478.
20. Lindenbach BD, Rice CM. Molecular biology of flaviviruses. *Adv Virus Res* 2003; **59:** 23–61.
21. Strauss JH, Strauss EG. Virus evolution: how does an enveloped virus make a regular structure? *Cell* 2001; **105:** 5–8.

SUPPLEMENTARY MATERIAL ONLINE

Figure S1. A high resolution version of Figure 1. A comparison of immunostaining between commercially available ZIKV antibodies in ZIKV-infected Vero cells (A–F), and uninfected Vero cells (G–L). Objective magnification, 40X

Figure S2. A high resolution version of Figure 2. Comparison of immunostaining between the commercially available ZIKV antibodies using ZIKV-infected case control (A–F), and uninfected CNS (G–L) tissue. Objective magnification, 20X

Figure S3. Cross-reactivity profile of commercially available ZIKV antibodies tested against dengue virus control cells [serogroups (sg) 1–4]. Immunostaining with ARI-A (images A–D), BIO-B (images E–H), GTX-C (images I–L), and GTX-D (images M–P). Objective magnification, 40X

Figure S4. Cross-reactivity profile of commercially available ZIKV antibodies tested against yellow fever virus, West Nile virus, Japanese encephalitis, and chikungunya virus. Immunostaining with ARI-A (images A–D), BIO-B (images E–H), GTX-C (images I–L), and GTX-D (images M–P). Objective magnification, 40X